Buffer–Induced Electrocatalytic Nitrite Reduction: Impact on Catalytic Rate and Product Selectivity.

Sheyda Partovi,[†] Evan Z. Dalton,[†] and Jeremy M. Smith[†*]

[†] Department of Chemistry, Indiana University, Bloomington, IN 47405, United States.

Abstract: The complex $[Co(CR)Br_2]^+$, where CR is the redox-active macrocycle 2,12-dimethyl-3,7,11,17-tetraazabicyclo-[11.3.1]-heptadeca-1(17),2,11,13,15-pentaene, is known as an electrocatalyst for the reduction of aqueous nitrite (NO_2^-). Here, we report that buffer induces a catalytic wave for NO_2^- reduction by $[Co(CR)Br_2]^+$, which occurs at a significantly more anodic potential than in unbuffered conditions. In addition, buffer increases the rate of electrocatalysis. This enhanced electrocatalytic activity is enabled by a number of buffering agents, with MOPS (3-(*N*-morpholino)propanesulfonic acid) showing the largest catalytic current. In addition to the greater catalytic activity, buffering agents influence the selectivity of the reduction products as well as catalyst longevity.

Keywords: electrocatalysis, buffer, nitrite reduction, hydroxylamine, ammonium

Introduction

Haber-Bosch ammonia (NH_3) enabled the world population to flourish by revolutionizing nitrogen fertilizer use in modern agriculture, providing enhanced food security to billions.[1] Excess ammonia is oxidized by soil bacteria into nitrate (NO_3^-) and nitrite (NO_2^-)[2] that are washed downstream into large water bodies worldwide, destabilizing the natural global N cycle. The increased nutrient levels in these waterbodies results in eutrophication that leads to hypoxia and ultimately to dead zones.[3] Remediating and rehabilitating these ecosystems is a large and expensive undertaking.[4] Decreasing nitrogen oxyanion accumulation is key to preventing the formation of hypoxic zones.

Electrocatalysis offers an appealing strategy for converting nitrogen oxyanions to benign or useful compounds. In previous work, our group has reported the electrocatalytic reduction of nitrogen oxyanions in aqueous solution using well-defined molecular complexes (Figure 1).[5-7] Among other design criteria, these studies have revealed the beneficial effects of intramolecular proton donors. More recently, we showed that phosphate buffer can activate electrocatalytic NO_2^- reduction in the otherwise catalytically–inactive complex $[Co(TIM)Br_2]^+$ (TIM = 2,3,9,10-tetramethyl-1,4,8,11-tetraazacyclotetradeca-1,3,8,10-tetraene), which we attributed to the ability of the buffer cation to act as an intermolecular proton donor.[8] The impact of buffer on electrocatalysis was further demonstrated in a preliminary electrochemical experiment for *trans*-$[Co(DIM)Br_2]^+$ (DIM = 2,3-dimethyl-1,4,8,11-tetraazacyclotetradeca-1,3-diene). In neutral unbuffered aqueous solution, this complex electrocatalytically reduces NO_2^- to ammonium (NH_4^+) with high Faradaic efficiency.[6] However, in pH 7 phosphate buffer, the product distribution changes to favor hydroxylamine (NH_2OH) as the major product.[9]

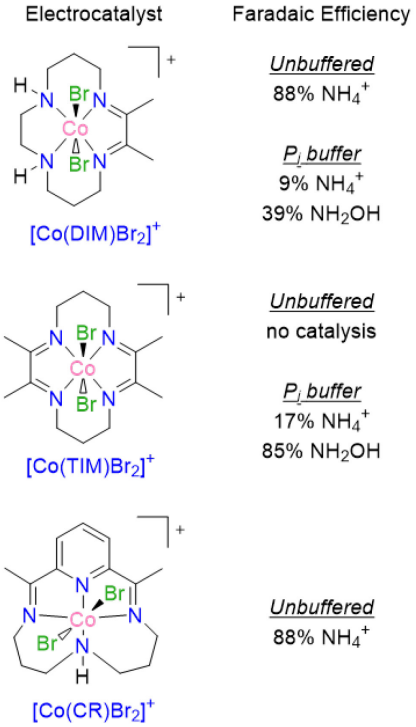

Figure 1: Cobalt macrocycle electrocatalysts for nitrite reduction in aqueous solution.[6, 8-10]

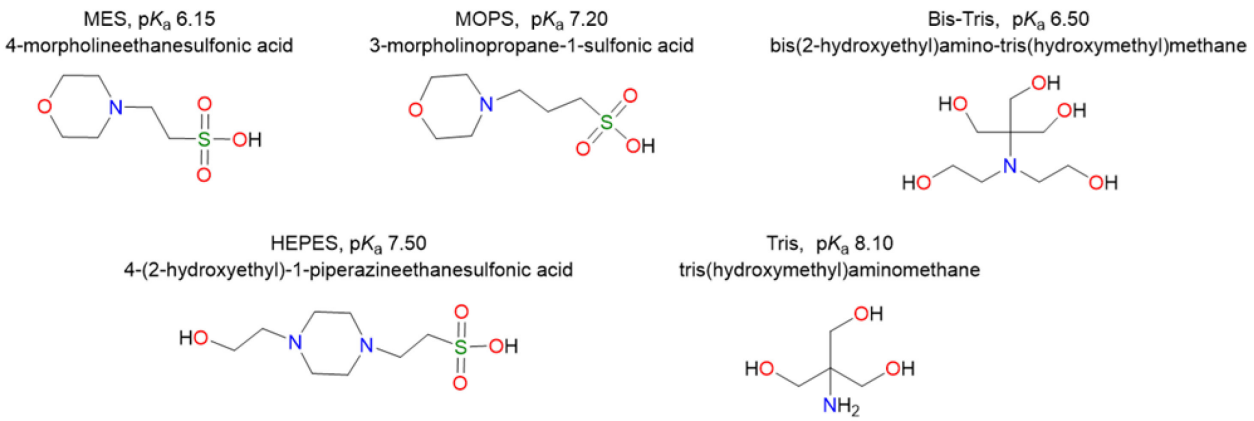

Figure 2: Structures of buffering agents investigated in this manuscript. All pK_a values are reported at 25 °C.

Other groups have investigated the electrocatalytic reduction of nitrite reduction in buffer. In studies done by Meyer et al., a number of electrocatalysts were active towards NO_2^- reduction in buffer, producing nitrous oxide (N_2O), N_2, and NH_2OH.[11-15] Su et al. explored Co and Fe porphyrins and found that NH_3 and NH_2OH were the major downstream reduction products.[16, 17] Although these are ostensibly NO_2^- reduction, the studies were done at acidic pH, therefore it is actually NO (nitric oxide) reduction. To the best of our knowledge, a systematic investigation on the effect of buffer on electrocatalytic NO_2^- reduction has not been reported.

Typically, a buffering agent is used to maintain solution pH as a non-interacting supporting electrolyte. However, buffer ions can be chemically non-innocent and participate in the electrocatalytic transformation, as demonstrated in a number of studies.[8, 18-38] For example, a series of studies by Meyer et al. have shown that the ability of a buffering agent to act as proton donor/acceptor can enhance reaction rates, modify the reaction pathway and avoid high energy intermediates.[30-38] In other studies, the strong proton donor ability of a buffering agent compensates for poor solvent proton donor capacity, thereby enabling electrochemical transformations.[8, 19, 25, 27]

In this work, we investigated the effect of buffer on the electrocatalytic reduction of NO_2^- using the cobalt complex, $[Co(CR)Br_2]^+$, where CR is the redox-active macrocycle 2,12-dimethyl-3,7,11,17-tetraazabicyclo-[11.3.1]-heptadeca-1(17),2,11,13,15-pentaene. We previously showed $[Co(CR)Br_2]^+$ can electrochemically reduce both NO_2^- and NO_3^- under aqueous conditions.[10] In this manuscript, we report that the addition of buffer leads to a new electrochemical process in the cyclic voltammogram (CV) of $[Co(CR)Br_2]^+$ in the presence of NO_2^-. This new process is associated with NO_2^- reduction and occurs with an onset potential that is over 460 mV more positive than that for NO_2^- reduction in unbuffered conditions.[39] Moreover, we show that the rate of electrocatalysis and product selectivity is influenced by buffering agent identity for a series with pK_a values close to 7 (Figure 2). Together, these results show the beneficial effects of buffer on both the overpotential and selectivity of electrocatalytic NO_2^- reduction.

Characterization of $[Co(CR)Br_2]^+$ in MOPS Buffer

The solution chemistry of $[Co(CR)Br_2]^+$ in 0.1 M MOPS (3-morpholinopropane-1-sulfonic acid) buffer (pH 7) is similar to that observed in unbuffered aqueous solution at neutral pH. As with unbuffered conditions, green $[Co(CR)Br_2]^+$ forms a yellow solution when dissolved in MOPS buffer, consistent with hydrolysis to provide a mixture of $[Co(CR)(OH)(OH_2)]^{2+}$ and $[Co(CR)(OH)_2]^+$.[10] As with unbuffered conditions, the CV of $[Co(CR)Br_2]^+$ in MOPS buffer reveals three electrochemical processes assigned to the $Co^{III/II}$, $Co^{II/I}$, and $CR/CR^{\cdot-}$ couples. The most notable difference between buffered and unbuffered conditions is that the $CR/CR^{\cdot-}$ process has a greater current response in MOPS buffer. (Figure 3a)

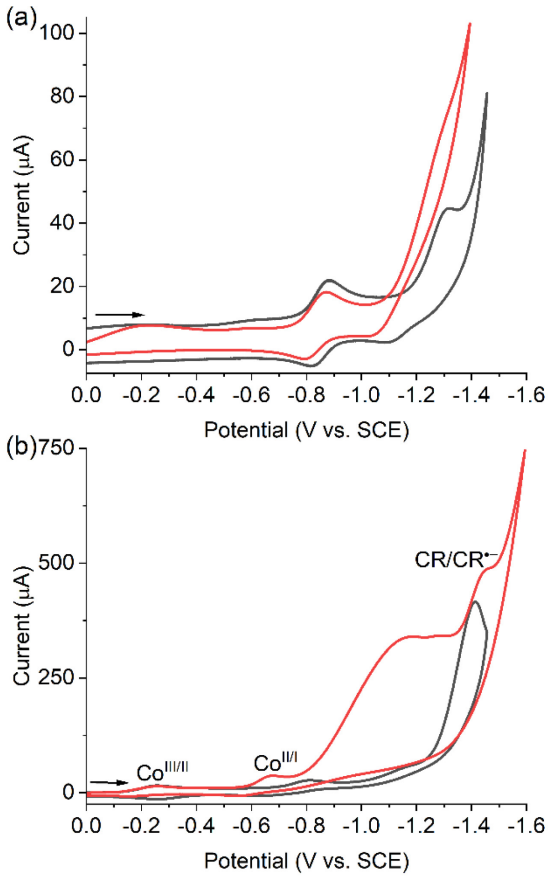

Figure 3: Cyclic voltammograms of 1 mM $[Co(CR)Br_2]^+$ in 0.1 M Na_2SO_4 (black) and 0.1 M pH 7 MOPS (red). a) without $NaNO_2$ and b) with 100 mM $NaNO_2$. Conditions: glassy carbon working electrode, Pt wire counter electrode, Ag/AgCl reference electrode*, 100 mV s^{-1}.*

Electrocatalytic NO_2^- Reduction in MOPS

Cyclic voltammetry reveals that the buffer has a beneficial impact on electrocatalytic NO_2^- reduction. Compared to unbuffered conditions, there is a slight increase (~67 μA) in the peak current associated with the electrocatalytic wave plateau at –1.44 V_{SCE}. More dramatically, a new electrocatalytic wave emerges, whose onset potential (~ –0.81 V_{SCE}) is over 460 mV more anodic than for unbuffered conditions (Figure 3b) The plateau current for this wave is also achieved at a more anodic potential (–1.16 V_{SCE} vs. –1.41 V_{SCE}), albeit with a lower current. As expected for NO_2^- reduction, the current increases with increasing $[NO_2^-]$ (Figure S2). These observations suggest that MOPS has a synergistic effect on electrocatalytic NO_2^- reduction by $[Co(CR)Br_2]^+$.

We investigated the effect of MOPS buffer concentration to better understand its role in electrocatalysis. At low buffer concentrations, the catalytic current initially increases with increasing [MOPS], however inhibition is observed at concentrations greater than ~0.75 M (Figure 4). Control experiments establish that ionic strength has no effect on electrocatalysis (Figure S3), suggesting the buffer ions play an intimate role in the reaction mechanism.

As has been previously shown, the dependence of the catalytic current on buffer concentration can be described according to a model in which inhibition is due to the buffer base (B) coordinating to the cobalt ion (Equation 1):

$$\left(\frac{i_{cat}}{i_{water}}\right)^2 = \frac{1+\frac{k_B[B]}{k_{water}}}{\left(1+\frac{K_{eq,1}[B]}{[NO_2^-]}+\frac{K_{eq,1}K_{eq,2}[B]^2}{[NO_2^-]^2}\right)^2} \qquad (1)$$

where i_{cat} and i_w are the catalytic currents observed in the presence and absence of buffer, respectively, k_{water} is the rate constant in the absence of buffer, k_B the rate constant in the presence of buffer, $K_{eq,1}$ the equilibrium constant for binding the first buffer base, and $K_{eq,2}$ the equilibrium constant binding the second buffer base.[8]

$Co(NO_2)_2 + B \rightleftarrows CoB(NO_2) + NO_2^-$

$CoB(NO_2) + B \rightleftarrows CoB_2 + NO_2^-$

According to this model, the rate of electrocatalysis increases by almost three orders of magnitude compared to unbuffered conditions, $k_B/k_{water} = 9.2(1) \times 10^2$ (Table S3).

We attribute the inhibiting effects of large buffer concentrations to the ability of the buffer base to bind cobalt in place of NO_2^- (and/or its reduction intermediates), as we have previously described for $[Co(TIM)Br_2]^+$.[8] By coordinating to the cobalt center, the buffer base hinders the binding of substrate and therefore decreases electrocatalytic activity.

We also assessed the effect of MOPS buffer on the NO_2^- reduction products by controlled potential electrolysis (CPE) experiments. Following 1 h electrolysis at –1.25 V_{SCE} in 0.75

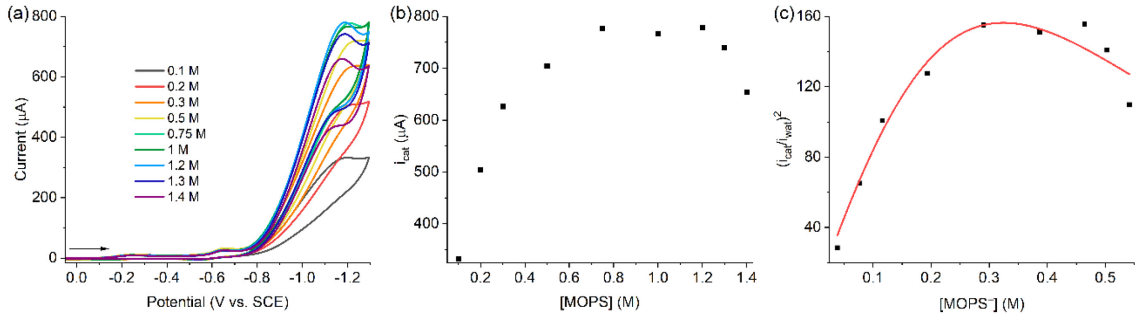

Figure 4: a) Cyclic voltammograms of 1 mM $[Co(CR)Br_2]^+$ in varying concentrations of MOPS buffer at pH 7 with 100 mM $NaNO_2$. Conditions: GC working electrode, Pt wire counter electrode, Ag/AgCl reference electrode, 100 mV s^{-1}. b) Plot of current (i_{cat}) at –1.20 V_{SCE} vs. buffer concentration. c) Plot of $(i_{cat}/i_{wat})^2$ vs. buffer base concentration fit with Eq. 1.

M MOPS, the primary reaction products are characterized to be NH_2OH (Faradaic efficiency 47±3 %) and NH_4^+ (Faradaic efficiency 30±5 %), as determined colorimetrically[40, 41] (Figure 5, Table S8). While trace H_2 and NO are formed, there is no evidence for the reductive formation of N_2O or NO_2 (Tables S6 and S7). The overall Faradaic efficiency is likely lowered by competitive reductive processes that are responsible for catalyst decomposition. It is notable that the product distribution differs from that observed for $[Co(CR)Br_2]^+$ in unbuffered aqueous media, where NH_4^+ is the only product of electrocatalytic reduction.[10] While the effect of buffer was not specifically investigated, it is worth noting that Bren et al.[19] and Su et al.[16] observe that NH_2OH is the more abundant NO_2^- reduction product in a variety of buffer solutions.

We suggest that there are two possible reasons for the change in product distribution to favor NH_2OH. Firstly, the buffer acid has the ability to act as a reservoir of protons, as dictated by the concentration of the conjugate acid, which may play a role in stabilizing NH_2OH as an intermediate, e.g., through hydrogen bonding. Secondly, the buffer conjugate base has the ability to act as a competitive ligand for NO_2^- and its reduction products, slowing its complete reduction to NH_4^+.

NO_2^- Electroreduction in Other Buffers

The synergistic effect of MOPS buffer on the electrocatalytic reduction of NO_2^- by $[Co(CR)Br_2]^+$ prompted us to investigate the impact of other buffers, specifically those that are able to buffer at pH 7 in aqueous solution (Figure 2). Here, we anticipated that the constant pH would allow us to obtain insights into the effects of buffering agent structure on electrocatalytic activity.

Table 1: Rate enhancement for nitrite reductions (k_B/k_W) as determined by Equation 1 for five buffers at pH 7.

Buffer	pK_a	k_B/k_W
MES	6.15	$1.4(7) \times 10^2$
Bis-Tris	6.50	$1.4(3) \times 10^2$
MOPS	7.20	$9.2(1) \times 10^2$
HEPES	7.50	$1.2(3) \times 10^3$
Tris	8.10	$2.6(4) \times 10^3$

The new electrocatalytic wave observed in MOPS buffer is also observed in the CVs of these other buffers. As with MOPS, current enhancement is observed at low buffer concentrations, but is inhibited at high concentrations. Fitting these data according to Eq. 1 reveals that the rate of catalysis is related to the pK_a of the buffer (Table 1), with increasing buffer pK_a correlating with faster rates of reaction. This suggests that the rate of electrocatalysis is determined by the ability of the buffer acid to act as a reservoir of protons, with higher pK_a translating to larger reservoirs.

We also investigated the effect of buffering agent on the reduction products. As informed by the studies described above (see also Figures S4-S7), CPE was conducted at buffer concentrations for which the maximum current response was observed (Table S8). In these studies, the applied potential was within 120 mV of that required to achieve the plateau current for the new

electrocatalytic wave (–1.25 V_{SCE} in all cases, see Figures S11a, S13a, S15a, S17a, and S19a).

It is notable that the combined Faradaic efficiency of NH_2OH and NH_4^+ after 1 h electrolysis is buffer dependent. Moreover, the combined NH_2OH and NH_4^+ Faradaic efficiency decreases as the buffer pK_a increases, suggesting that larger proton reservoirs are better able to induce catalyst decomposition.

Similar to our observations in MOPS buffer, the primary nitrogen-containing products for most of the buffers are NH_2OH and NH_4^+ (Figure 5a and Table S8). Only trace H_2 and NO are observed (Tables S6 and S7). The exception is Tris, where NH_4^+ formation is not observed, possibly because of competitive binding of this primary amine.

Lower concentrations of MOPS decrease the Faradaic efficiency for NH_4^+ formation (Table S9), although the product distribution appears to be relatively insensitive to buffer concentration in this concentration range (similar results were observed for two concentrations of Bis-Tris buffer). More dramatically, NH_4^+ formation is suppressed when electrolysis is conducted in 0.75 M MOPS containing 10 mol% Tris buffer. Under these conditions, NH_2OH is generated as the sole NO_2^- reduction product.

Prolonged electrolysis (5 h) decreases the overall Faradaic efficiency for NH_2OH and NH_4^+ formation in all buffers. In addition, we find that CVs taken post-electrolysis show a diminished current for both the electrochemical and electrocatalytic processes (Figures S12b, S14b, S16b, S18b, and S20b). Together with the corresponding spectral changes, this suggests that the lower Faradaic efficiencies are the result of catalyst decomposition.[42] It is notable that the relative decrease in efficiency is not solely dependent on the buffer pK_a. Specifically, there is a dramatic decrease in the overall Faradaic efficiency for NH_2OH and NH_4^+ in Bis-Tris and Tris, whereas a more modest decrease is observed for the other buffers (Figure 5b).

These results suggest that the ability of the buffer ions to form metal complexes has the most dramatic effect on the overall NH_2OH and NH_4^+ Faradaic efficiency. It is notable that the Bis-Tris and Tris buffers, which are associated with the lowest overall NH_2OH and NH_4^+ Faradaic efficiency, are well known to form metal complexes.[43-46] Tris is the least sterically encumbered which can allow for tighter binding with the catalyst. By contrast, MES and MOPS are poor ligands on the basis of isothermal titration calorimetry experiments.[47] Binding constant studies suggest that HEPES is a better ligand than MES and MOPS,[47-50] but poorer than Bis-Tris and Tris.[51] The combined data suggests an order of metal binding ability: Tris ≈ Bis-Tris > HEPES > MOPS ≈ MES. In the case of these weaker coordinating buffers, the overall Faradaic efficiency for NH_2OH and NH_4^+ decreases with increasing buffer pK_a, although the effect is relatively modest. The extremely poor NH_2OH Faradaic efficiency for Tris may also be related to its pK_a.

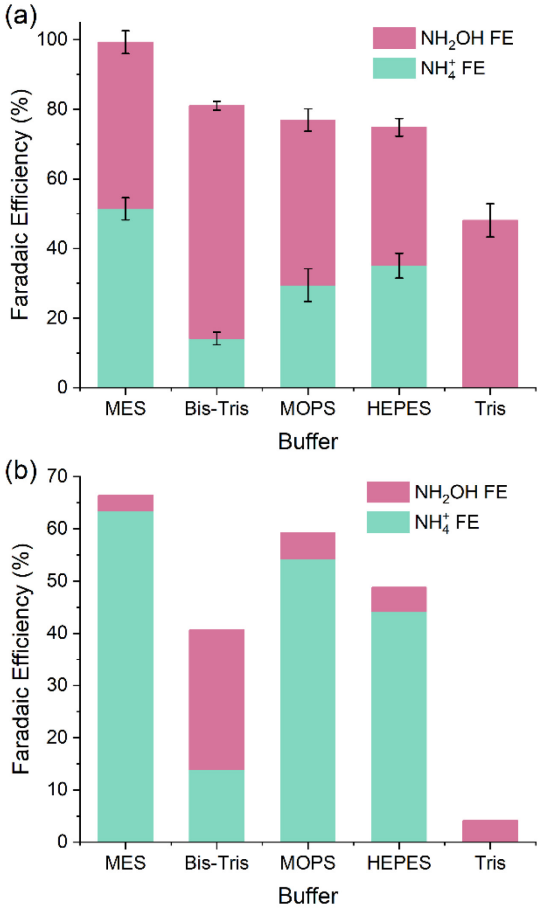

Figure 5: Faradaic efficiency of the buffers following (a) 1 h and (b) 5 h CPE, respectively. All CPE were held at –1.25 V_{SCE}.

It is also notable that prolonged CPE also decreases the Faradaic efficiency for NH_2OH (Figure 5b) in all buffers. In the case of MES,

MOPS and HEPES, there is a corresponding increase in Faradaic efficiency for NH_4^+, suggesting that the NH_2OH observed after 1 h CPE is further reduced by $[Co(CR)Br_2]^+$. On the other hand, there is no change in the Faradaic efficiency for NH_4^+ in the case of Bis-Tris and Tris buffers. Indeed, we never observe the formation of NH_4^+ in Tris buffer. In light of the lower combined NH_2OH and NH_4^+ Faradaic efficiency for these two buffers, we suggest that the buffer anions outcompete NH_2OH for binding to the cobalt center (Figure 6), thereby preventing further reduction to NH_4^+, as well as facilitating decomposition of the catalyst.

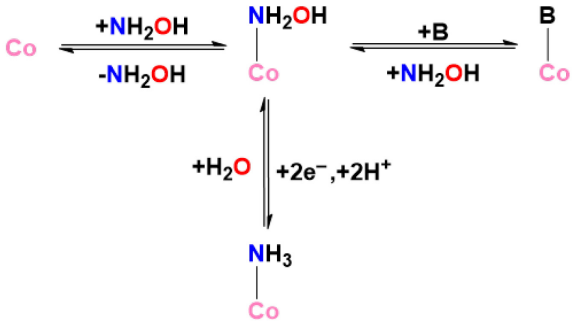

Figure 6: Competitive buffer binding prevents further reduction of hydroxylamine.

Conclusions

In this work, we observe that buffer induces a new pathway for the electrocatalytic reduction of NO_2^- by the cobalt macrocycle complex, $[Co(CR)Br_2]^+$. The relative rate of reduction is dependent on the ability of the buffer to supply protons, as characterized by its pK_a. Specifically, at the same pH, the buffering agent with the highest pK_a will provide the largest reservoir of protons, leading to the fastest rates.

We also observe that coordinating ability of the buffer has an impact on NO_2^- reduction electrocatalysis. Buffer ions that are known to bind well with transition metal ions (i.e., Bis-Tris and Tris) are associated with lower overall Faradaic efficiencies; also have higher selectivity for the formation of NH_2OH. While there are a handful of cases demonstrating the ability of buffer to act as a proton donor or acceptor,[30-38, 52] our results suggest the coordinating ability of the buffer anion as an additional variable in electrocatalytic schemes, notably as a method for controlling product selectivity in multielectron conversions.

Corresponding Author

Jeremy M. Smith

smith962@indiana.edu

Notes

The authors declare no competing financial interests.

Supporting Information

Full experimental details, materials, and methods, including additional cyclic voltammograms, controlled potential electrolyses, and product characterization (pdf).

Acknowledgements

SP and JMS gratefully acknowledge funding from the NSF (CHE-2102442). EZD acknowledges support from Indiana Space Grant Consortium and NSF (AGS–1352375 and CHE–2305078). We would like to thank Jonathan D. Raff for insightful conversations.

References:

(1) Smil, V., *Enriching the Earth: Fritz Haber, Carl Bosch, and the Transformation of World Food Production*. The MIT Press: 2000.

(2) Matassa, S.; Batstone, D. J.; Hülsen, T.; Schnoor, J.; Verstraete, W., Can Direct Conversion of Used Nitrogen to New Feed and Protein Help Feed the World? *Environ. Sci. Technol.* **2015**, *49*, 5247-5254.

(3) Selman, M.; Sugg, Z.; Greenhalgh, S.; Diaz, R., Eutrophication and Hypoxia in Coastal Areas: A Global Assessment of the State of Knowledge. *WRI Policy Note* **2008**, *1*, 6.

(4) Kemp, W. M.; Testa, J. M.; Conley, D. J.; Gilbert, D.; Hagy, J. D., Temporal responses of coastal hypoxia to nutrient loading and physical controls. *Biogeosciences* **2009**, *6*, 2985-3008.

(5) Xu, S.; Ashley, D. C.; Kwon, H.-Y.; Ware, G. R.; Chen, C.-H.; Losovyj, Y.; Gao, X.; Jakubikova, E.; Smith, J. M., A Flexible, Redox-Active Macrocycle Enables the Electrocatalytic Reduction of Nitrate to Ammonia by a Cobalt Complex. *Chem. Sci.* **2018**, *9*, 4950-4958.

(6) Xu, S.; Kwon, H.-Y.; Ashley, D. C.; Chen, C.-H.; Jakubikova, E.; Smith, J. M., Intramolecular Hydrogen Bonding Facilitates Electrocatalytic Reduction of Nitrite in Aqueous Solutions. *Inorg. Chem.* **2019**, *58*, 9443-9451.
(7) Braley, S. E.; Ashley, D. C.; Kulesa, K. M.; Jakubikova, E.; Smith, J. M., Electrode-adsorption activates *trans*-$[Cr(cyclam)Cl_2]^+$ for electrocatalytic nitrate reduction. *Chem. Commun.* **2020**, *56*, 603-606.
(8) Braley, S. E.; Kwon, H.-Y.; Xu, S.; Dalton, E. Z.; Jakubikova, E.; Smith, J. M., Buffer Assists Electrocatalytic Nitrite Reduction by a Cobalt Macrocycle Complex. *Inorg. Chem.* **2022**, *61*, 12998-13006.
(9) Braley, S. E. Rational Electrocatalytic System Design in the Pursuit of Mechanistic Understanding of Nitrogen Oxyanion Reduction. Ph.D., Indiana University, United States -- Indiana, 2022.
(10) Partovi, S.; Xiong, Z.; Kulesa, K. M.; Smith, J. M., Electrocatalytic Reduction of Nitrogen Oxyanions with a Redox-Active Cobalt Macrocycle Complex. *Inorg. Chem.* **2022**, *61*, 9034-9039.
(11) Barley, M. H.; Rhodes, M. R.; Meyer, T. J., Electrocatalytic reduction of nitrite to nitrous oxide and ammonia based on the N-methylated, cationic iron porphyrin complex $[Fe^{III}(H_2O)(TMPyP)]^{5+}$. *Inorg. Chem.* **1987**, *26*, 1746-1750.
(12) Murphy, W. R., Jr.; Takeuchi, K.; Barley, M. H.; Meyer, T. J., Mechanism of reduction of bound nitrite to ammonia. *Inorg. Chem.* **1986**, *25*, 1041-1053.
(13) Rhodes, M. R.; Barley, M. H.; Meyer, T. J., Electrocatalytic reduction of nitrite ion by edta complexes of iron(II) and ruthenium(II). *Inorg. Chem.* **1991**, *30*, 629-635.
(14) Rhodes, M. R.; Meyer, T. J., Electrocatalytic reduction of nitrite using simple coordination complexes of iron and ruthenium. *Inorg. Chem.* **1988**, *27*, 4772-4774.
(15) Barley, M. H.; Takeuchi, K.; Murphy, W. R.; Meyer, T. J., Iron porphyrin-based electrocatalytic reduction of nitrite to ammonia. *J. Chem. Soc., Chem. Commun.* **1985**, 507-508.
(16) Cheng, S.-H.; Su, Y. O., Electrocatalysis of Nitric Oxide Reduction by Water-Soluble Cobalt Porphyrin. Spectral and Electrochemical Studies. *Inorg. Chem.* **1994**, *33*, 5847-5854.
(17) Chen, S.-M.; Su, Y. O., Electrocatalytic reduction of nitric oxide to ammonia by water-soluble iron porphyrin. *J. Electroanal. Chem.* **1990**, *280*, 189-194.
(18) Alvarez-Hernandez, J. L.; Sopchak, A. E.; Bren, K. L., Buffer pK_a Impacts the Mechanism of Hydrogen Evolution Catalyzed by a Cobalt Porphyrin-Peptide. *Inorg. Chem.* **2020**, *59*, 8061-8069.
(19) Stroka, J. R.; Kandemir, B.; Matson, E. M.; Bren, K. L., Electrocatalytic Multielectron Nitrite Reduction in Water by an Iron Complex. *ACS Catal.* **2020**, *10*, 13968-13972.
(20) Le, J. M.; Alachouzos, G.; Chino, M.; Frontier, A. J.; Lombardi, A.; Bren, K. L., Tuning Mechanism through Buffer Dependence of Hydrogen Evolution Catalyzed by a Cobalt Mini-enzyme. *Biochemistry* **2020**, *59*, 1289-1297.
(21) Alvarez-Hernandez, J. L.; Han, J. W.; Sopchak, A. E.; Guo, Y.; Bren, K. L., Linear Free Energy Relationships in Hydrogen Evolution Catalysis by a Cobalt Tripeptide in Water. *ACS Energy Lett.* **2021**, *6*, 2256-2261.
(22) Alvarez-Hernandez, J. L.; Salamatian, A. A.; Han, J. W.; Bren, K. L., Potential- and Buffer-Dependent Selectivity for the Conversion of CO_2 to CO by a Cobalt Porphyrin-Peptide Electrocatalyst in Water. *ACS Catal.* **2022**, 14689-14697.
(23) Schneider, C. R.; Lewis, L. C.; Shafaat, H. S., The good, the neutral, and the positive: buffer identity impacts CO_2 reduction activity by nickel(II) cyclam. *Dalton Trans.* **2019**, *48*, 15810-15821.
(24) Behnke, S. L.; Manesis, A. C.; Shafaat, H. S., Spectroelectrochemical investigations of nickel cyclam indicate different reaction mechanisms for electrocatalytic CO_2 and H^+ reduction. *Dalton Trans.* **2018**, *47*, 15206-15216.
(25) Wang, D.; Groves, J. T., Efficient water oxidation catalyzed by homogeneous cationic cobalt porphyrins with critical roles for the buffer base. *Proc. Natl. Acad. Sci. U.S.A.* **2013**, *110*, 15579-15584.
(26) Wang, D.; Groves, J. T., Energy Landscape for the Electrocatalytic Oxidation of Water by a Single-Site Oxomanganese(V) Porphyrin. *Inorg. Chem.* **2022**, *61*, 13667-13672.

(27) van Langevelde, P. H.; Engbers, S.; Buda, F.; Hetterscheid, D. G. H., Elucidation of the Electrocatalytic Nitrite Reduction Mechanism by Bio-Inspired Copper Complexes. *ACS Catal.* **2023**, *13*, 10094-10103.
(28) Zhou, J.; Han, S.; Yang, R.; Li, T.; Li, W.; Wang, Y.; Yu, Y.; Zhang, B., Linear Adsorption Enables NO Selective Electroreduction to Hydroxylamine on Single Co Sites. *Angew. Chem. Int. Ed.* **2023**, *n/a*, e202305184.
(29) Medina-Ramos, J.; Oyesanya, O.; Alvarez, J. C., Buffer Effects in the Kinetics of Concerted Proton-Coupled Electron Transfer: The Electrochemical Oxidation of Glutathione Mediated by $[IrCl_6]_2^-$ at Variable Buffer pK_a and Concentration. *J. Phys. Chem. C* **2013**, *117*, 902-912.
(30) Chen, Z.; Concepcion, J. J.; Hu, X.; Yang, W.; Hoertz, P. G.; Meyer, T. J., Concerted O atom-proton transfer in the O-O bond forming step in water oxidation. *Proc. Natl. Acad. Sci. U.S.A.* **2010**, *107*, 7225-7229.
(31) Vannucci, A. K.; Alibabaei, L.; Losego, M. D.; Concepcion, J. J.; Kalanyan, B.; Parsons, G. N.; Meyer, T. J., Crossing the divide between homogeneous and heterogeneous catalysis in water oxidation. *Proc. Natl. Acad. Sci. U.S.A.* **2013**, *110*, 20918-20922.
(32) Paul, A.; Hull, J. F.; Norris, M. R.; Chen, Z.; Ess, D. H.; Concepcion, J. J.; Meyer, T. J., Multiple Pathways for Benzyl Alcohol Oxidation by $Ru^{V}{=}O^{3+}$ and $Ru^{IV}{=}O^{2+}$. *Inorg. Chem.* **2011**, *50*, 1167-1169.
(33) Tamaki, Y.; Vannucci, A. K.; Dares, C. J.; Binstead, R. A.; Meyer, T. J., One-Electron Activation of Water Oxidation Catalysis. *J. Am. Chem. Soc.* **2014**, *136*, 6854-6857.
(34) Chen, Z.; Vannucci, A. K.; Concepcion, J. J.; Jurss, J. W.; Meyer, T. J., Proton-coupled electron transfer at modified electrodes by multiple pathways. *Proc. Natl. Acad. Sci. U.S.A.* **2011**, *108*, E1461-E1469.
(35) Murphy, C. F.; Dongare, P.; Weatherly, S. C.; Gagliardi, C. J.; Thorp, H. H.; Meyer, T. J., Proton-Coupled Electron Transfer in the Oxidation of Guanosine Monophosphate by $Ru(bpy)_3^{3+}$. *J. Phys. Chem. C* **2018**, *122*, 24830-24837.
(36) Fecenko, C. J.; Thorp, H. H.; Meyer, T. J., The Role of Free Energy Change in Coupled Electron−Proton Transfer. *J. Am. Chem. Soc.* **2007**, *129*, 15098-15099.
(37) Coggins, M. K.; Zhang, M.-T.; Chen, Z.; Song, N.; Meyer, T. J., Single-Site Copper(II) Water Oxidation Electrocatalysis: Rate Enhancements with HPO_4^{2-} as a Proton Acceptor at pH 8. *Angew. Chem. Int. Ed.* **2014**, *53*, 12226-12230.
(38) Fecenko, C. J.; Meyer, T. J.; Thorp, H. H., Electrocatalytic Oxidation of Tyrosine by Parallel Rate-Limiting Proton Transfer and Multisite Electron−Proton Transfer. *J. Am. Chem. Soc.* **2006**, *128*, 11020-11021.
(39) See SI for details on the assignment of the onset potential.
(40) Weatherburn, M. W., Phenol-hypochlorite reaction for determination of ammonia. *Anal. Chem.* **1967**, *39*, 971-974.
(41) Frear, D. S.; Burrell, R. C., Spectrophotometric Method for Determining Hydroxylamine Reductase Activity in Higher Plants. *Anal. Chem.* **1955**, *27*, 1664-1665.
(42) Catalyst deactivation is supported by cyclic voltammetry and can be seen in Figure S21.
(43) Scheller, K. H.; Abel, T. H. J.; Polanyi, P. E.; Wenk, P. K.; Fischer, B. E.; Sigel, H., Metal Ion/Buffer Interactions: Stability of Binary and Ternary Complexes Containing 2-[Bis(2-hydroxyethyl)amino]-2(hydroxymethyl)-1,3-propanediol (Bistris) and Adenosine 5′-Triphosphate (ATP). *Eur. J. Biochem.* **1980**, *107*, 455-466.
(44) Inomata, Y.; Gochou, Y.; Nogami, M.; Howell, F. S.; Takeuchi, T., Characterization of ternary bivalent metal complexes with bis(2-hydroxyethyl)iminotris(hydroxymethy)methane (Bis–Tris) and the comparison of five crystal structures of Bis–Tris complexes. *J. Mol. Struct.* **2004**, *702*, 61-70.
(45) Fischer, B. E.; Häring, U. K.; Tribolet, R.; Sigel, H., Metal Ion/Buffer Interactions: Stability of Binary and Ternary Complexes Containing 2-Amino-2(hydroxymethyl)-1,3-propanediol (Tris) and Adenosine 5′-Triphosphate (ATP). *Eur. J. Biochem.* **1979**, *94*, 523-530.
(46) Kotila, S.; Valkonen, J., Copper (II) complexes of 2-amino-2-hydroxymethyl-1,3-propanediol. Part 2: Synthesis, structure and thermal behavior of cis-[2-amino-2-hydroxymethyl-1,3-propanediol(1, 3-)-

O,O',N][2-amino-2-hydroxymethyl-1,3-propanediolato(1-)O,N]nitratocopper(II), [Cu($C_4H_{10}NO_3$)($C_4H_{11}NO_3$)(NO_3)], and cis-[2-amino-2-hydroxymethyl-1, 3-propanediol(1, 3-)-O, O', N][2-amino-2-hydroxymethyl-1,3-propanediolato(1, 3-)-O, O', N]copper(II) sodium bis(perchlorate), [Cu($C_4H_{10}NO_3$)($C_4H_{11}NO_3$)]Na(ClO_4)$_2$. *Acta Chem. Scand.* **1993**, *47*, 957-964.
(47) Xiao, C.-Q.; Huang, Q.; Zhang, Y.; Zhang, H.-Q.; Lai, L., Binding thermodynamics of divalent metal ions to several biological buffers. *Thermochim. Acta* **2020**, *691*, 178721.
(48) Mash, H. E.; Chin, Y.-P.; Sigg, L.; Hari, R.; Xue, H., Complexation of Copper by Zwitterionic Aminosulfonic (Good) Buffers. *Anal. Chem.* **2003**, *75*, 671-677.
(49) Jiang, H.; Ma, J.-F.; Zhang, W.-L.; Liu, Y.-Y.; Yang, J.; Ping, G.-J.; Su, Z.-M., Metal–Organic Frameworks Containing Flexible Bis(benzimidazole) Ligands. *Eur. J. Inorg. Chem.* **2008**, *2008*, 745-755.
(50) Babel, L.; Bonnet-Gómez, S.; Fromm, K. M., Appropriate Buffers for Studying the Bioinorganic Chemistry of Silver(I). *Chemistry* **2020**, *2*, 193-202.
(51) Ferreira, C. M. H.; Pinto, I. S. S.; Soares, E. V.; Soares, H. M. V. M., (Un)suitability of the use of pH buffers in biological, biochemical and environmental studies and their interaction with metal ions – a review. *RSC Advances* **2015**, *5*, 30989-31003.
(52) Huynh, M. H. V.; Meyer, T. J., Proton-Coupled Electron Transfer. *Chem. Rev.* **2007**, *107*, 5004-5064.